Dong Wen-Kui (Orcid ID: 0000-0003-1249-5808)

Highly efficient detection of Cu^{2+} and $B_4O_7^{2-}$ based on a recyclable asymmetric salamo-based probe in aqueous media

Xin Xu[1] | Ya-Juan Li[1] | Tao Feng[1] | Wen-Kui Dong[1,*] | Yu-Jie Ding[2,**]

[1] *School of Chemical and Biological Engineering, Lanzhou Jiaotong University, Lanzhou, Gansu 730070, China*

[2] *College of Biochemical Engineering, Anhui Polytechnic University, Wuhu 241000, Chinaa*

Abstract

The asymmetric salamo-based probe molecule (**H_2L**) was synthesized and characterized structurally. When DMF / H_2O (9 : 1) was used as the solvent, it was shown the probe **H_2L** has high sensitivity to Cu^{2+}. Using high-resolution mass spectrometry and theoretical calculation, it was found that the probe **H_2L** can form a more stable complex (1:1) with Cu^{2+}, the minimum detection limit (LOD) of **H_2L** for Cu^{2+} was calculated as 9.95×10^{-8} M. In addition, the probe **H_2L** can also be used to identify $B_4O_7^{2-}$ under the same detection condition and the minimum detection limit (LOD) of **H_2L** for $B_4O_7^{2-}$ was calculated as 4.98×10^{-7} M. At the same time, the DFT theoretical calculation further proved the flexibility of the probe **H_2L**. Through the action of EDTA, the probe **H_2L** had a cyclic ability to recognize Cu^{2+}, and showed a better response in the physiological pH range, and the probe **H_2L** had the characteristics of fast recognition speed and high efficiency. In addition, the probe **H_2L** tested the test paper of Cu^{2+} and $B_4O_7^{2-}$, and the effect was more obvious. Meanwhile, the probe **H_2L** can be used to quantitatively detect Cu^{2+} in water samples.

K E Y W O R D S: Asymmetric salamo-based probe, synthesis, reversible detection, PET

* Corresponding author. Fax: +86 931 4938703.

** Corresponding author.

E-mail addresses: dongwk@126.com (W.-K. Dong), yujieding123@163.com (Y.-J. Ding).

This article has been accepted for publication and undergone full peer review but has not been through the copyediting, typesetting, pagination and proofreading process which may lead to differences between this version and the Version of Record. Please cite this article as doi: 10.1002/bio.3932

This article is protected by copyright. All rights reserved.

mechanism, DFT calculation[1]

1 | INTRODUCTION

Copper ions are widely found in nature and are essential micronutrients for human health [1]. Although their content is very small, the human body will be abnormal once it is lacking [2]. Copper ions are the structural components and active centers of some enzymes in the body, and also act as activators to affect the activity of enzyme [3– 6]. It has an important influence on the development and function of blood, central nervous system, immune system, hair, skin, bone tissue, brain, liver and heart [7–10]. In addition, copper often appears in the form of complexes, and it has a variety of forms, usually can be used as a small molecule catalyst, which makes copper complexes widely used in industrial production [11]. However, in industrial production and human environment [12–14], excessive copper ions will lead to environmental pollution and abnormal body functions, which becomes very important for the rapid and accurate detection of copper ions [15].

Borax is a very important boron-containing mineral and a boron compound [16–18]. Borax has a wide range of uses and can be used as a cleaning agent, a cosmetic, an insecticide, and other boron compounds [19,20]. Although boron is a necessary trace element in the human body, the content is too low and too high, which will have a damaging effect [21–23]. Adding borax to food may cause cumulative damage to the human body [24,25]. Long-term excessive intake of boron has toxic effects on human reproduction, development and endocrine system. It is widely used as a food additive in various countries in the world, but because it is highly toxic, although it is very necessary to detect borax [26]. At present, the detection of borax is mainly carried out by the neutralization titration method, the steps of this method are relatively cumbersome and the cost is relatively high [27,28]. Therefore, the development of a fluorescent probe for quantitative analysis of $B_4O_7^{2-}$ becomes extremely important for living organisms and the environment [29–31]. However, the use of salamo-based ligands for fluorescence detection of $B_4O_7^{2-}$ is very rare.

This article is protected by copyright. All rights reserved.

People are devoted to designing and synthesizing low-cost and fast-response high-sensitivity fluorescent probes for identifying water, environment, and organisms to quickly and effectively detect heavy metal ions and more toxic anions [32–35]. Salamo-based compouns and their derivatives are the most versatile chelating ligands in inorganic and organometallic chemistry [36–39]. The salamo-based ligands are coordinated by oxygen and nitrogen atoms, and have basically similar coordination characteristics with a wide range of metal ions [40–43], and have the advantages of relatively simple preparation method, relatively easy structure modification and good selectivity [44–46]. The catalysts [47,48], magnetic materials [49], electrochemistry [50,51], luminescent materials [52,53], antibacterial activities [54,55] and probe properties of salamo-based complexes make them more widely used [56–58]. In this study, a new fluorescent probe was discovered for the detection of $B_4O_7^{2-}$ and Cu^{2+}, which is very rare, and the detection of $B_4O_7^{2-}$ and Cu^{2+} can be achieved by its fluorescence intensity [59–61].

2 | E X P E R I M E N T A L

2.1 | Materials and methods

The reagents and solvents selected are analytical grade reagents from the Cologne Reagent Plant in Chengdu. All metal salts used in the cation test were of the formula $M(NO_3)_n \cdot xH_2O$, while the sodium salt was used in the anion experiment. ^1H and ^{13}C NMR spectra were recorded in $CDCl_3$ solution at room temperature on a Bruker AV 500 MHz spectrometer at 500 and 126 MHz, respectively. The melting point was obtained using a micro melting point apparatus manufactured by Beijing Tyco Instrument Co., Ltd. Fluorescence spectroscopy was performed on an F-7000 FL 220-240V spectrophotometer from Hitachi, Tokyo, Japan. All pH measurements were made using a pH-10C digital pH meter.

The probe **H_2L** (3.30 mg, 0.01 mmol) was dissolved in 10 mL of DMF: H_2O (9:1, V / V) solution to a final concentration of 1×10^{-3} mol/L. The arrangement of anionic and cationic salts was also 1×10^{-2} mol/L, respectively. All tests were performed in Tris-HCl solvent with pH = 7.23. The fluorescence test was performed with a 1 cm adaptive cuvette at room temperature. A fluorescence spectrometer was used to monitor the change in fluorescence

This article is protected by copyright. All rights reserved.

intensity (λ_{ex} = 310 nm, slit width 10/10 nm).

All quantum calculations are run using Gaussian 09, using density functional theory (DFT), using the Becke's three parameter hybrid method by using the Becke88exchange functional and LYP correlation functional (B3LYP), and selecting the 6-31G (d, p) basis set for geometric optimization. The molecular electrostatic potential (MEP) and molecular orbital analysis of the probe was done with Multiwfn3.7, and the three-dimensional space map was drawn using VMD software.

2.2 | Synthesis of the probe H_2L

6-Methoxy-2,2′-[ethylenedioxybis(nitrilomethylidyne)]diphenol (**H_2L**) was synthesized according to a similar method previously reported [62,63]. The reaction procedure for the synthesis of the salamo-based probe (**H_2L**) was shown in Scheme 1. Finally, a white powder was obtained in a yield of 77.9% (Based on 2-hydroxybenzaldehyde). M. p.: 72-74 °C. Anal. calcd. for $C_{17}H_{18}N_2O_5$: C, 61.81; H, 5.49; N, 8.48. Found: C, 61.96; H, 5.54; N, 8.36. ^{1}H NMR (500 MHz, $CDCl_3$): δ 9.74 (s, 2H), 8.24 (s, 2H), 7.29 (d, J = 7.1 Hz, 1H), 7.16 (d, J = 6.1 Hz, 1H), 6.97 (d, J = 8.2 Hz, 1H), 6.91 (d, J = 3.6 Hz, 2H), 6.86 (s, 1H), 6.82 (dd, J = 7.8, 1.7 Hz, 1H), 4.48 (s, 4H), 3.91 (s, 3H). (Figure S1). ^{13}C NMR (126 MHz, $CDCl_3$): δ 157.46 (C), 152.33 (CH=N), 152.01 (CH=N), 148.20 (C), 147.13 (C), 131.39 (CH), 130.94 (CH), 122.44 (CH), 119.57 (d, CH), 116.78 (CH), 116.49 (C), 116.20 (C), 113.57 (CH), 73.14 (CH_2), 72.95 (CH_2), 56.21 (CH_3). (Figure S2).

3 | RESULTS AND DISCUSSION

3.1 | Solvent selection

3.1.1. Solvent effect

In order to study the effect of solvents on the fluorescence intensity of the probe **H_2L**, more than ten commonly used solvents (MeOH, EtOH, DMK, THF, ACN, Py, TCM, DCM, PhH, EA, DMF and DMSO) were selected for testing, and a suitable solvent was selected for subsequent testing of the probe **H_2L**. The best emission wavelength of benzene with the

This article is protected by copyright. All rights reserved.

lowest polarity was selected as the emission wavelength of the test, and the fluorescence spectra of the probe **H_2L** were tested for the above solvents at the same emission wavelength (Figure 1). The experimental phenomenon indicated that the probe **H_2L** shows the strongest fluorescence in DMF solvent. Therefore, DMF solvent was selected as the best solvent for the test.

3.1.2. Water-containing system study

The influence of the aqueous organic mixing system on the probe **H_2L** needs to be further studied, and the organic mixing system with the optimal water content was selected as the solvent for subsequent experiments. As the water content increased, the fluorescence intensity weakened relatively. When the water content in the system reached 90%, a large amount of flocculent precipitates was generated in the solution, and the fluorescence was quenched (Figure 2). Therefore, the performance of the probe **H_2L** was selected in a 90% DMF aqueous solution and used as a solvent for subsequent experiments.

3.2 | Fluorescence response of H_2L to various metal cations

*3.2.1. The probe **H_2L** response to cations*

Based on the above experimental basis, the detection of cation recognition by the probe **H_2L** was carried out in the solvent system of DMF: H_2O (9:1, V / V). When Cu^{2+} was added to the probe **H_2L** solution, the color of the solution changed significantly. Under a normal light source, the color of the solution changed from the original light yellow to bright brown. Under the irradiation of a 365 nm UV lamp, the solution of the probe **H_2L** was bright blue, and the color of the solution disappeared after the addition of Cu^{2+} (Figure 3).

At an excitation wavelength of 330 nm, the probe **H_2L** solution showed a strong fluorescence emission band at approximate 387 nm. Excessive cations were added to the probe **H_2L** solution, and the experimental results found that the fluorescence of the probe

This article is protected by copyright. All rights reserved.

H_2L solution was completely quenched only when Cu^{2+} was added. In addition, after added Zn^{2+}, Mn^{2+} and Fe^{3+}, the fluorescence of the probe **H_2L** solution also quenched to some extent, but these results did not affect the recognition of Cu^{2+} by the probe **H_2L** (Figure 4a).

The specificity and sensitivity of the probe **H_2L** to Cu^{2+} recognition was further studied through fluorescence anti-interference experiments (Figure 4b). After added various metal ions (Li^+, Na^+, K^+, Mg^{2+}, Ca^{2+}, Sr^{2+}, Ba^{2+}, Cr^{3+}, Mn^{2+}, Fe^{3+}, Co^{2+}, Ni^{2+}, Cu^{2+}, Zn^{2+}, Pb^{2+}, Ag^+, Cd^{2+}, Al^{3+} and Hg^{2+}) to the probe **H_2L** solution respectively, the fluorescence intensity of the solution hardly changed, and then a certain amount of Cu^{2+} was added to the metal ion-containing solution respectively, and the fluorescence intensity of the solution was quenched. The results of anti-interference experiment are consistent with the results of Irving-Williams sequence, the L-Cu^{2+} complex is more stable in the corresponding complexes formed by transition metal ions and the ligands containing N coordination atoms. Interestingly, the fluorescence intensity of L-Cu^{2+} solution decreases to a lower value after added Pb^{2+}, which can be attributed to the closing of the fluorescence group of the probe **H_2L**, resulting in a decrease in the fluorescence of L-Cu^{2+} [64]. The experimental results showed that other metal ions have little effect on the recognition of Cu^{2+} by the probe **H_2L**, which reflected the specificity of the probe **H_2L**.

Subsequently, a fluorescence titration experiment was performed to check the binding ability of **H_2L** to Cu^{2+}. In 2 mL of Tris-HCl buffer solution (1×10^{-5} mol/L), added 20 μL of **H_2L** solution, and added Cu^{2+} solution to it. As the amount of Cu^{2+} continues to increased, the fluorescence intensity of the solution gradually weakened. When 1.0 equivalent of Cu^{2+} solution was added, the fluorescence of the solution was completely quenched, and after exceeding 1.0 equivalent, the fluorescence intensity of the solution no longer changes, as shown in Figure 4c. The titration results indicated that the probe **H_2L** formed a 1: 1 stable complex and Cu^{2+}. At the same time, we also draw the working curve of the probe molecule **H_2L** to identify Cu^{2+}, which further proved that the ratio of **H_2L** to Cu^{2+} is 1: 1 (Figure S3). In addition, LOD (9.95×10^{-8} M) and LOQ (3.32×10^{-7} M) were calculated (Figure S4a) [7,35]. According to the Hill equation (Figure S4b) [15], the binding constant K of **H_2L** and Cu^{2+} was estimated to be 1.36×10^{9} M^{-1}, the calculation results showed that the probe **H_2L**

This article is protected by copyright. All rights reserved.

has a high binding capacity for Cu^{2+}.

*3.2.2. Recognition mechanism of the probe **H_2L** for Cu^{2+}*

Based on the above experimental results and theoretical basis, the recognition mechanism of the probe **H_2L** to Cu^{2+} was explored. High-resolution mass spectrometry was performed on the copper complex (Figure S5). From the high-resolution mass spectrum, the highest peak could be seen at 394.14, the molecular weight of the probe **H_2L** was 330.34, which was exactly the same as the molecular weight of the different copper atoms (64). This result was consistent with the above titration part, and the probe **H_2L** formed a 1: 1 complex with Cu^{2+} (Scheme 2).

In addition, the theoretical calculation of the probe **H_2L** and its copper(II) complex was carried out [38,39]. The structure of the optimized probe **H_2L** and copper(II) complex was shown in Figure 5. The HOMO and LUMO orbits of the probe **H_2L** showed that there were high electron densities on the N and O atoms, which indicated that the cavity formed by N and O atoms was easy to coordinated with Cu^{2+}. When Cu^{2+} was added, the phenolic hydroxyl group of the probe **H_2L** was completely deprotonated, and Cu^{2+} coordinated with its phenolic oxygen and oxime nitrogen atoms and formed a new copper(II) complex. The energy gap difference between the HOMO and LUMO of the copper complex was 6.09655 eV, which was lower than the energy gap difference between the HOMO and LUMO of the probe **H_2L** (6.8227 eV), which indicated that L-Cu^{2+} was more stable, which further indicated that the addition of Cu^{2+} caused fluorescence quenched.

*3.2.3. Reversible test of **H_2L** recognition of Cu^{2+}*

Through the study of the mechanism, the reversibility of the probe **H_2L** for Cu^{2+} recognition was further studied. EDTA is a more commonly used complexometric agent. In this process, EDTA was selected as the probe **H_2L** to recognize the reversibility of Cu^{2+}. By alternately adding Cu^{2+} and EDTA, the fluorescence change of the probe **H_2L** in the "off-on-off" mode was achieved. As shown in Figure 6, the fluorescence emission of the probe **H_2L**

This article is protected by copyright. All rights reserved.

showed alternating fluorescence quenching and enhancement in at least three cycles, and the fluorescence loss was small, indicating that the recognition process of Cu^{2+} by the probe **H_2L** was reversible.

Finally, the previously reported literatures were compared with the binding constants and detection lines of Cu^{2+} and $B_4O_7^{2-}$ identified in this work. From Table 1, we can see that our probe **H_2L** is superior to them [5,6,9,10,26,61].

3.3 | Fluorescence response of H_2L to various anions

*3.3.1. The probe **H_2L** response to anions*

In order to further explored the response of the probe **H_2L** to anions (F^-, Cl^-, Br^-, I^-, HPO_4^{2-}, $H_2PO_4^-$, $P_2O_7^{4-}$, S^{2-}, OAc^-, SO_4^{2-}, CO_3^{2-}, HCO_3^-, CN^-, ClO_4^- and $B_4O_7^{2-}$), it was studied by added different anions to the probe **H_2L** solution, as shown in Figure 7a. When the $B_4O_7^{2-}$ was added, the fluorescence intensity of the probe **H_2L** solution was quenched, different from identifying Cu^{2+}, new peaks appeared at 392 and 452 nm during the identification of $B_4O_7^{2-}$, and it could be seen in the illustration that their solution disappeared under a 365 nm UV lamp. However, after added other anions, the fluorescence intensity of the probe **H_2L** solution did not change significantly. Among them, only when F^- was added, the fluorescence intensity had a small changed and weakened. The experimental results showed that the probe **H_2L** had a highly specific recognition of $B_4O_7^{2-}$ in common anions.

The effect of other anions on the recognition of $B_4O_7^{2-}$ by the probe **H_2L** was further studied through anti-interference experiments, as shown in Figure 7b. After separately added other anions to the probe **H_2L** solution (F^-, Cl^-, Br^-, I^-, HPO_4^{2-}, $H_2PO_4^-$, $P_2O_7^{4-}$, S^{2-}, OAc^-, SO_4^{2-}, CO_3^{2-}, HCO_3^-, CN^- and ClO_4^-), the fluorescence intensity of the solution did not change significantly, and then separately added $B_4O_7^{2-}$ solution to the above solution, the fluorescence intensity of the solution was quenched immediately. The experimental results indicated that the presence of anions had little effect on the probe **H_2L** recognized $B_4O_7^{2-}$.

In addition, for the cause of detect the binding capacity of **H_2L** and $B_4O_7^{2-}$, a fluorescence titration experiment was performed, and $B_4O_7^{2-}$ solution was added dropwise to the **H_2L** solution until the end point. As shown in Figure 7c, as the amount of $B_4O_7^{2-}$ was continuously added, the fluorescence intensity of the probe **H_2L** solution was continuously

This article is protected by copyright. All rights reserved.

weakened. When added to 5.0 equivalents, the fluorescence of the solution was completely quenched, and the fluorescence intensity no longer changed after continued addition. The experimental results showed that the probe **H_2L** formed a 1: 5 coordination with $B_4O_7^{2-}$. In addition, LOD (4.98×10^{-7} M) and LOQ (1.66×10^{-6} M) were calculated (Figure S6a). By the Hill equation (Figure S6b), it was estimated that the binding constant *K* of **H_2L** and $B_4O_7^{2-}$ was 3.72×10^8 M^{-1}, which indicated that **H_2L** had a higher binding ability to $B_4O_7^{2-}$.

3.3.2. $B_4O_7^{2-}$ Recognition mechanism

For the cause of further exploring the reaction mechanism and predicting the attack site and charge density of the chemical reaction, electrostatic potential (ESP) analysis was performed on the probe **H_2L** [65]. As shown in Figure 8, the values of different electrostatic potentials on the molecular surface are marked with different colors, where red represents a positive electrostatic potential, blue represents a negative electrostatic potential, and the white part represents the zero-potential area. The negative potential that appears near the benzene ring is mainly due to the delocalized π bond contained in it, and the negative potential is also concentrated near the N and O atoms. This is mainly because these two atoms can act as electron donor, there by forming other new complex.

Borate could be hydrolyzed to boric acid was the main reason led to fluorescence quenched:

$$\left[B_4O_5(OH)_4\right]^{2-} + 5H_2O \rightleftharpoons 4H_3BO_3 + 2OH^- \rightleftharpoons 2H_3BO_3 + 2B(OH)_4^-$$

Due to the electron donor nature of the probe **H_2L**, the special configuration of boric acid entered the **H_2L** conjugated system, which led to photo-induced electron transfer (PET), which changed the optical properties of the system and quenched fluorescence [26]. On the other hand, the most stable configuration of boric acid was the C3h point group, and the C3h point group of boric acid molecules was conducive to the expansion of the intermolecular hydrogen bonding system, which could form a periodic structure in the two-dimensional

This article is protected by copyright. All rights reserved.

plane, which also made boric acid molecules were in a state of aggregation in solution, caused the occurrence of aggregation-caused quenching (ACQ).

3.4 | Effect of pH on the probe H_2L

In order to investigate whether the probe **H_2L** can be practically used in a physiological environment, the pH range of **H_2L**, L-Cu^{2+} and L-$B_4O_7^{2-}$ were tested (Figure 9). When the pH value was 1~3, the acidity of the solution was too strong, which might cause the probe **H_2L** to lose activity, and led to low fluorescence intensity. When the pH is between 4~12, the fluorescence value of the probe **H_2L** increased, which indicated that the applicable range of **H_2L** was between pH = 4~12. After added Cu^{2+} to the probe **H_2L**, it was found that the fluorescence intensity in the pH range of 1~3 was consistent with that of the probe **H_2L**, and the fluorescence intensity was quenched in the pH range of 4~10. The range of applicable pH for the probe **H_2L** to recognized Cu^{2+} was 4~10. Similarly, it can be observed that the range of suitable pH for **H_2L** to recognized $B_4O_7^{2-}$ was 4~9. From the above conclusions, the probe **H_2L** was an excellent probe that could detect Cu^{2+} and $B_4O_7^{2-}$ in a physiological environment, and had excellent application prospect.

3.5 | Time response of the probe H_2L

In order to further understand whether the probe **H_2L** has the ability of rapid recognition, the effect of time on recognition was studied (Figure 10). Within 10 seconds of adding Cu^{2+} to the **H_2L** solution, the fluorescence of the solution was quenched, and within the next 1 minute, the fluorescence intensity no longer changed, which indicated that within 10 seconds, the probe **H_2L** could perform on Cu^{2+} quickly identified. According to the same method as above, a time response test was performed on the probe **H_2L** recognition $B_4O_7^{2-}$, and it was found that the probe **H_2L** recognition of $B_4O_7^{2-}$ can also be within 10 seconds. It was indicated that the probe **H_2L** has the characteristics of high efficiency and rapid recognition of Cu^{2+} and $B_4O_7^{2-}$.

This article is protected by copyright. All rights reserved.

3.6 | Practical application of the probe H_2L

In order to evaluate the practical application of the probe **H_2L** in life, it was used to detect the Cu^{2+} content in different water samples [15]. Added quantitative Cu^{2+} to different water samples, and analyzed the test samples by standard addition method used fluorescence spectroscopy. As shown in Figure 11 and Table 2, the Cu^{2+} content in tap water, river water, and rain water is 2.3, 5.2, and 7.6 μM, respectively. Repeat the test 3 times, and the relative standard deviation is within 5%. The experimental results showed that the probe **H_2L** can be used for the quantitative detection of Cu^{2+} in different water samples.

In order to facilitate the rapid detection of Cu^{2+} and $B_4O_7^{2-}$ in the probe **H_2L** in daily life [13,66], corresponding test strip test strips were made, as shown in Figure 12. Dip the dilute hydrochloric acid treated filter paper in a DMF: H_2O (9:1, V / V) solution with a concentration of 1.0×10^{-3} mol/L **H_2L** for loading. After the load was uniformed, place the test paper in a vacuum drying-box for low temperature dried, and used the dried test paper for the detection of Cu^{2+} content, the test paper was blue under an ultraviolet lamp before the test. After the Cu^{2+} solution was dropped on the test paper strip, the color of the blue color of the test strip would disappear within 10 seconds. After the solution of other metal ions was added dropwise on the test paper, the test paper still showed blue under the UV lamp. After added Cu^{2+} to the test paper again, the fluorescence of the test paper test strip disappeared under the UV lamp. The same test was performed on $B_4O_7^{2-}$ according to a similar detection method, and the experimental effect was quite impressive. This test strip was more convenient for daily life detection, and made it more widely used.

4 | CONCLUSIONS

In this work, a new salamo-based probe **H_2L** was synthesized, which can be used to detect Cu^{2+} and $B_4O_7^{2-}$ in the physiological range, with a fast detection rate and simple preparation. Through high-resolution mass spectrometry, it was found that the probe **H_2L** can coordinate with Cu^{2+} to form a new copper(II) complex. Further DFT theoretical calculations indicated that the newly formed complex has a stable structure, which led to fluorescence

This article is protected by copyright. All rights reserved.

quenching. The recognition of $B_4O_7^{2-}$ was mainly due to the fact that $B_4O_7^{2-}$ is prone to hydrolysis, and the formed H_3BO_3 had a unique structure. Through the ESP analysis of the probe **H_2L**, it can be seen that the N and O atoms of the probe **H_2L** had a stronger ability to electrons donor, and photo-induced electron transfer would occur. H_3BO_3 affects the electron cloud density of **H_2L**, which caused fluorescence quenching. Finally, the probe **H_2L** can measure the content of Cu^{2+} in different water samples in real life, and obtained a test strip for rapid testing of Cu^{2+} and $B_4O_7^{2-}$.

DECLARATIONS OF INTEREST:

The authors declare no conflict of interest.

ACKNOWLEDGEMENTS

This work was supported by the National Natural Science Foundation of China (21761018) and the Program for Excellent Team of Scientific Research in Lanzhou Jiaotong University (201706), both of which are gratefully acknowledged.

Accepted Article

This article is protected by copyright. All rights reserved.

REFERENCES

[1] Z. Y. Gündüz, C. Gündüz, C. Özpınar, O. A. Urucu, *Spectrochim. Acta A* **2015**, *136*, 1679.

[2] R. Khisamov, T. Sukhikh, D. Bashirov, A. Ryadun, S. Konchenko, *Molecules* **2020**, *25*, 2428.

[3] K. Y. Ryu, J. J. Lee, J. A. Kim, D. Y. Park, C. Kim, *RSC Adv.* **2016**, *6*, 16586.

[4] A. Kenaan, F. Brunel, J. M. Raimundo, A. M. Charrier, *Sens. Actuators B* **2020**, *316*,128147.

[5] Y. Zhang, L. Li, J. P. Wang, L. H. Jia, R. Yang, X. F. Guo, *Spectrochim. Acta A* **2020**, *230*, 118030.

[6] M. Tian, H. He, B. B. Wang, X. Wang, Y. Liu, F. L. Jiang, *Dyes Pigments.* **2019**, *165*, 383.

[7] Y. Q. Pan, X. Xu, Y. Zhang, Y. Zhang, W. K. Dong, *Spectrochim. Acta A* **2020**, *229*, 117927.

[8] M. Yu, Y. Zhang, Y. Q. Pan, L. Wang, *Inorg. Chim. Acta* **2020**, *509*, 119701.

[9] A. Mohammadi, B. Khalili, A. S. Haghayegh, *Spectrochim. Acta A* **2019**, *222*, 117193.

[10] P. K. Muwal, A. Nayal, M. K. Jaiswal, P. S. Pandey, *Tetrahedron Lett.* **2018**, *59*, 29.

[11] Y. Zhang, Y. Q. Pan, M. Yu, X. Xu, W. K. Dong, *Appl. Organomet. Chem.* **2019**, *33*, e5240.

[12] C. Li, X. T. Han, S. S. Mao, S. O. Aderinto, X. K. Shi, K. S. Shen, H. L. Wu, *Coloration Technol.* **2018**, *134*, 230.

[13] C. Long, J. H. Hu, P. W. Ni, Z. Y. Yin, Q. Q. Fu, *New J. Chem.* **2018**, *42*, 17056.

[14] P. X. Pei, J. H. Hu, P. W. Ni, C. Long, J. X. Su, Y. Sun, *RSC Adv.* **2017**, *7*, 46832.

[15] L. Wang, Z. L. Wei, Z. Z. Chen, C. Liu, W. K. Dong, Y. J. Ding, *Microchem. J.* **2020**, *155*, 104801.

[16] J. Li, Z. Liu, Y. Wang, R. Wang, *J. Alloys Compd.* **2020**, *834*, 155150.

[17] H. Morito, S. Shibano, T. Yamada, T. Ikeda, M. Terauchi, R.V. Belosludov, H. Yamane, *Solid State Sci.* **2020**, *102*, 106166.

[18] M. Chen, O. Dollar, K. Shafer-Peltier, S. Randtke, S. Waseem, E. Peltier, *Water Res.* **2020**, *170*, 115362.

This article is protected by copyright. All rights reserved.

[19] K. Wang, T. Yin, H. Zhou, X. Liu, J. Deng, S. Li, C. Lu, X. Chen, *J. Eur. Ceram. Soc.* **2020**, *40*, 381.

[20] F. Spadaro, A. Rossi, S. N. Ramakrishna, E. Lainé, P. Woodward, N. D. Spencer, *Langmuir.* **2018**, *34*, 2219.

[21] L. A. L. Dias, W. A. Alves, *J. Mol. Liq.* **2019**, *289*, 111152.

[22] S. Tursunbadalov, L. Soliev, *J. Chem. Eng. Data.* **2018**, *63*, 598.

[23] C. Bugra, K. Emirhan, D. Fatma, *Ceram. Int.* **2018**, *44*, 14264.

[24] K. G. Yves, T. Chen, J. T. Aladejana, Z. Wu, Y. Xie, *ACS Omega.* **2020**, *5*, 8784.

[25] A. Vera, J. L. Moreno, C. Garcia, D. Morais, F. Bastida, *Sci. Total Environ.* **2019**, *685*, 564.

[26] L. M. Pu, X. Y. Li, J. Hao, Y. X. Sun, Y. Zhang, H. T. Long, W. K. Dong, *Sci. Rep.* **2018**, *8*, 14058.

[27] P. C. Yin, Q. F. Niu, Q. X. Yang, L. X. Lan, T. D. Li, *Tetrahedron* **2019**, *75*, 130687.

[28] G. Kuz'micheva, R. Svetogorov, I. Kaurova, *J. Solid State Chem.* **2020**, *288*, 121393.

[29] X. Ding, Y. Gu, Q. Li, B. H. Kim, Q. Wang, J. Huang, *Ceram. Int.* **2020**, *46*, 13225.

[30] X. Cui, J. Wang, M. Wen, X. Dai, K. Miao, K. Wang, K. Zhang, *Ceram. Int.* **2020**, *46*, 9854.

[31] F. Risplendi, F. Raffone, L. C. Lin, J. C. Grossman, G. Cicero, *J. Phys. Chem. C.* **2020**, *124*, 1438.

[32] Q. P. Kang, X. Y. Li, L. Wang, Y. Zhang, W. K. Dong, *Appl. Organomet. Chem.* **2019**, *33*, e5013.

[33] S. Z. Zhang, J. Chang, H. J. Zhang, Y. X. Sun, Y. Wu, Y. B. Wang, *Chin. J. Inorg. Chem.* **2020**, *36*, 503.

[34] L. Wang, Z. L. Wei, C. Liu, W. K. Dong, J. X. Ru, *Spectrochim. Acta A* **2020**, *239*, 118496.

[35] L. Z. Liu, L. Wang, M. Yu, Q. Zhao, Y. Zhang, Y. X. Sun, W. K. Dong, *Spectrochim. Acta A* **2019**, *222*, 117209.

[36] L. S. Kostenko, I. I. Tomashchuk, T. V. Kovalchuk, O. A. Zaporozhets, *Appl. Clay. Sci.* **2019**, *172*, 49.

This article is protected by copyright. All rights reserved.

[37] X. X. An, Q. Zhao, H. R. Mu, W. K. Dong, *Crystals* **2019**, *9*, 101.

[38] H. R. Mu, X. X. An, C. Liu, Y. Zhang, W. K. Dong, *J. Struct. Chem.* **2020**, *61*, 1218.

[39] C. Liu, X. X. An, Y. F. Cui, K. F. Xie, W. K. Dong, *Appl. Organomet. Chem.* **2020**, *34*, e5272.

[40] Q. Zhao, X. X. An, L. Z. Liu, W. K. Dong, *Inorg. Chim. Acta* **2019**, *490*, 6.

[41] X. X. An, Z. Z. Chen, H. R. Mu, L. Zhao, *Inorg. Chim. Acta* **2020**, *511*, 119823.

[42] L. Z. Liu, M. Yu, X. Y. Li, Q. P. Kang, W. K. Dong, *Chin. J. Inorg. Chem.* **2019**, *35*, 1283.

[43] X. Y. Dong, Q. Zhao,, Z. L. Wei, H. Zhang, H. R. Mu, W. K. Dong, *Molecules* **2018**, *23*, 1006.

[44] H. R. Mu, M. Yu, L. Wang, Y. Zhang, Y. J. Ding, *Phosphorus Sulfur Silicon Relat. Elem.* **2020**, *195*, 730.

[45] J. H. Hu, Y. Sun, J. Qi, Q. Li, T. B. Wei, *Spectrochim. Acta A* **2017**, *175*, 125.

[46] Z. L. Wei, L. Wang, J. F. Wang, W. T. Guo, Y. Zhang, W. K. Dong, *Spectrochim. Acta A* **2020**, *228*, 117775.

[47] X. Y. Li, Q. P. Kang, C. Liu, Y. Zhang, W. K. Dong, *New J. Chem.* **2019**, *43*, 4605.

[48] Q. P. Kang, X. Y. Li, Z. L. Wei, Y. Zhang, W. K. Dong, *Polyhedron* **2019**, *165*, 38.

[49] X. Y. Dong, Q. P. Kang, X. Y. Li, J. C. Ma, W. K. Dong, *Crystals* **2018**, *8*, 139.

[50] K. S. Shen, S. S. Mao, X. K. Shi, F. Wang, Y. L. Xu, S. O. Aderinto, H. L. Wu, *Luminescence* **2018**, *33*, 54.

[51] S. Sucheta, E. Peter, P. Jürgen, *Opt. Express.* **2018**, *26*, 3443.

[52] J. Hao, X. Y. Li, Y. Zhang, W. K. Dong, *Materials* **2018**, *11*, 523.

[53] Y. D. Peng, F. Wang, L. Gao, W. K. Dong. *J. Chin. Chem. Soc.* **2018**, *65*, 893.

[54] Y. Q. Pan, Y. Zhang, M. Yu, Y. Zhang, L. Wang, *Appl. Organomet. Chem.* **2020**, *34*, e5441.

[55] M. Y. Ma, Z. Zhang, Z. N. Zhao, Q. L. Liao, Z. Kang, F. F. Gao, X. Zhao,Y. Zhang, *Nano Energy* **2019**, *66*, 104105.

[56] L. W. Zhang, Y. Zhang, Y. F. Cui, M. Yu, W. K. Dong, *Inorg. Chim. Acta* **2020**, *506*, 119534.

This article is protected by copyright. All rights reserved.

[57] Y. Zhang, L. Z. Liu, Y. D. Peng, N. Li, W. K. Dong, *Transit. Met. Chem.* **2019**, *44*, 627.

[58] Y. X. Sun, Y. Q. Pan, X. Xu, Y. Zhang, *Crystals* **2019**, *9*, 607.

[59] J. Chang, S. Z. Zhang, Y. Wu, H. J. Zhang, Y. X. Sun, *Transit. Met. Chem.* **2020**, *45*, 279.

[60] K. B. A. Ahmed, M. Sengan, S. K. P, A. Veerappan, *Sens. Actuators B* **2016**, *233*, 431.

[61] C. Liu, Z. L. Wei, H. R. Mu, W. K. Dong, Y. J. Ding, *J. Photochem. Photobio. A* **2020**, *397*, 112569.

[62] X. Y. Dong, Q. Zhao, Q. P. Kang, X. Y. Li, W. K. Dong, *Crystals* **2019**, *8*, 230.

[63] Y. Zhang, M. Yu, Y. Q. Pan, Y. Zhang, L. Xu, X. Y. Dong, *Appl. Organomet. Chem.* **2019**, *34*, e5442.

[64] C.A. Huerta-Aguilar, T. Pandiyan, N. Singh, N. Jayanthi, *Spectrochim. Acta A* **2015**, *146*, 142.

[65] G. Singh, J. Sindhu, Manisha, V. Kumar, V. Sharma, S. K. Sharma, S. K. Mehta, M. H. Mahnashi, A. Umar, R. Kataria, *J. Mol. Liq.* **2019**, *296*, 111814.

[66] L. Wang, Y. Q. Pan, J. F. Wang, Y. Zhang, Y. J. Ding, *J. Photochem. Photobiol. A* **2020**, *400*, 112719.

Accepted Article

This article is protected by copyright. All rights reserved.

Biographies

Xin Xu is currently pursuing her master's degree in the School of Chemical and Biological Engineering at Lanzhou Jiaotong University, China. She obtained her bachelor's degree in the School of Chemistry and Chemical Engineering of Jining University, China, in 2018.

Ya-Juan Li is currently pursuing her master's degree in the School of Chemical and Biological Engineering at Lanzhou Jiaotong University, China. She obtained a bachelor's degree from the School of Chemical Engineering, Tianshui Normal University, China in 2018.

Tao Feng is currently pursuing her master's degree in the School of Chemical and Biological Engineering at Lanzhou Jiaotong University, China. He received a bachelor's degree from the College of Chemical Engineering, Shanxi Datong University, China in 2018.

Wen-Kui Dong received his PhD degree in 1998 from Lanzhou University, China. He is a professor in the School of Chemical and Biological Engineering at Lanzhou Jiaotong University. His current research interests are focusing on the chemistry of functional supramolecular complexes, materials and new products, as well as processes and applications of environmental chemical engineering.

Yu-Jie Ding received her PhD degree in 2013 from Nanjing University, China; She is an associate professor in College of Biochemical Engineering at Anhui Polytechnic University, her current research interesting is the synthesis and application of upconversion luminescence nanomaterials.

Accepted Article

This article is protected by copyright. All rights reserved.

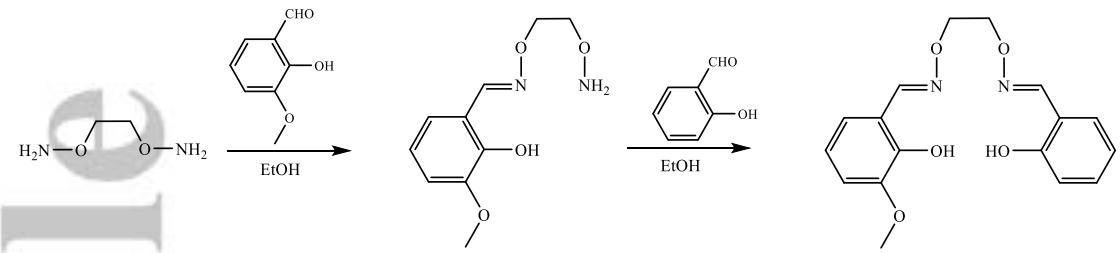

S C H E M E 1 Synthetic route to **H_2L**.

Accepted Article

This article is protected by copyright. All rights reserved.

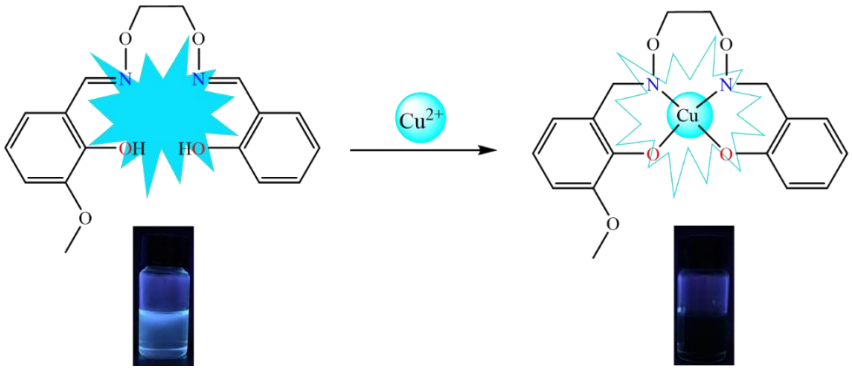

S C H E M E 2. Possible mechanism of Cu^{2+} recognition by probe **H_2L**.

Accepted Article

This article is protected by copyright. All rights reserved.

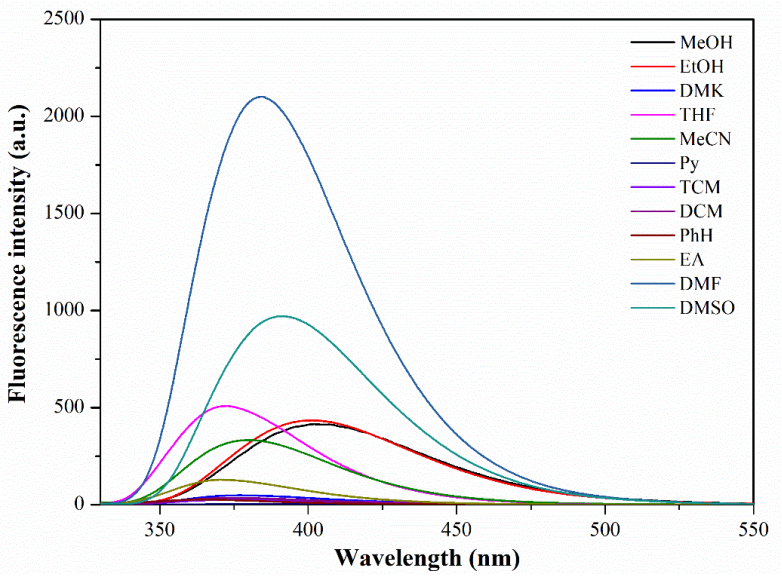

F I G U R E 1 Fluorescence intensities of **H_2L** measured under different solvents.

Accepted Article

This article is protected by copyright. All rights reserved.

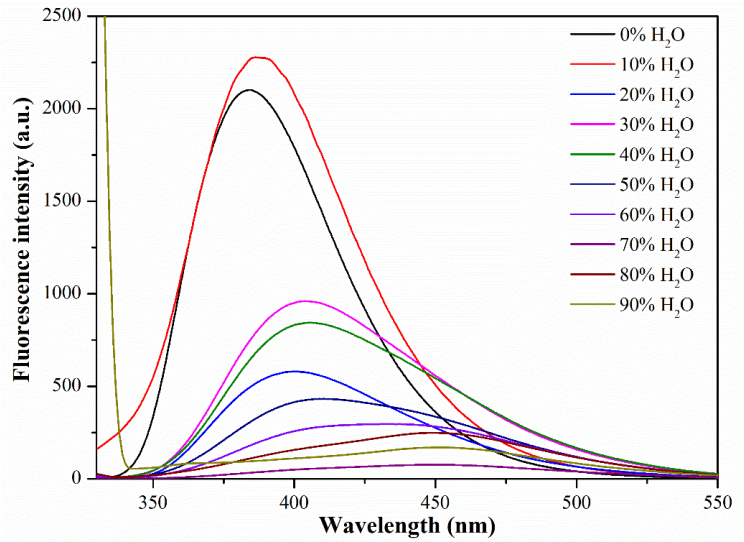

F I G U R E 2 Spectra of **H_2L** solutions (DMF) measured in different proportions of water.

Accepted Article

This article is protected by copyright. All rights reserved.

F I G U R E 3 Comparison of the probe **H_2L** and L-Cu^{2+} solution under normal light (left), and comparison between **H_2L** and L-Cu^{2+} solution under 365nm UV lamp (right).

Accepted Article

This article is protected by copyright. All rights reserved.

Accepted Article

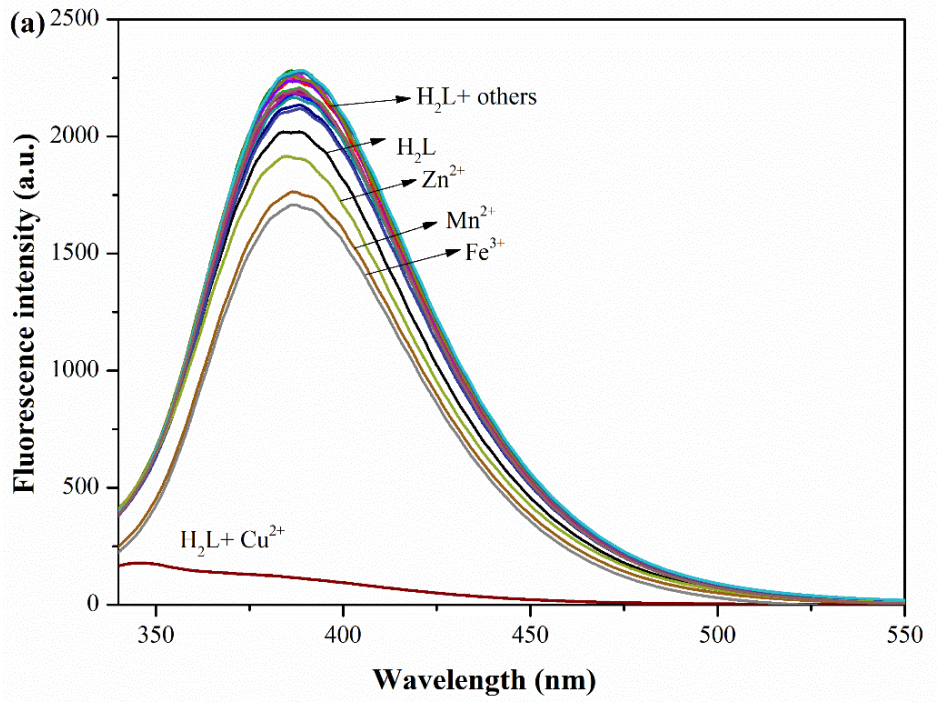

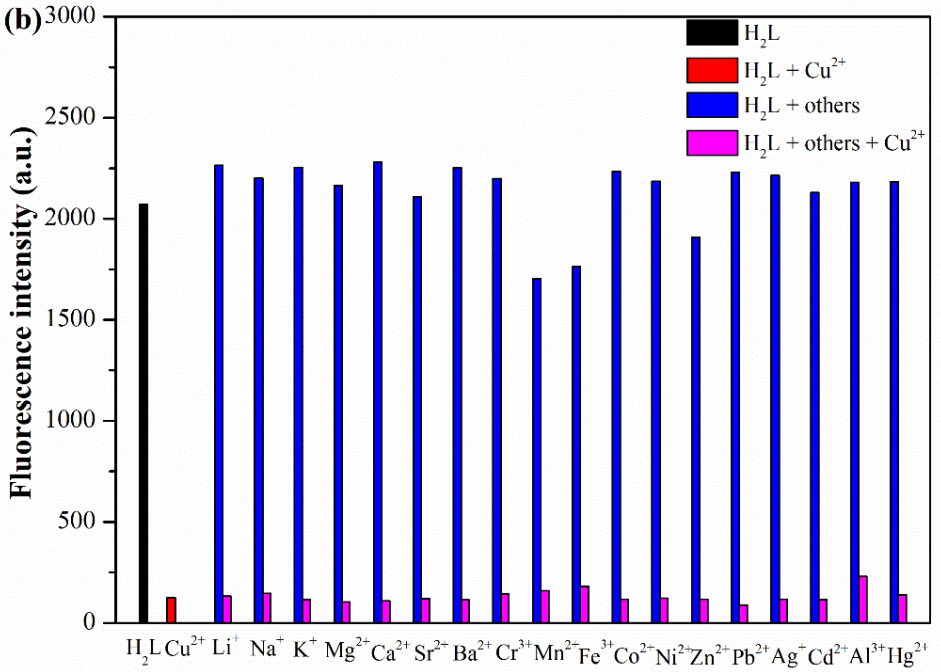

This article is protected by copyright. All rights reserved.

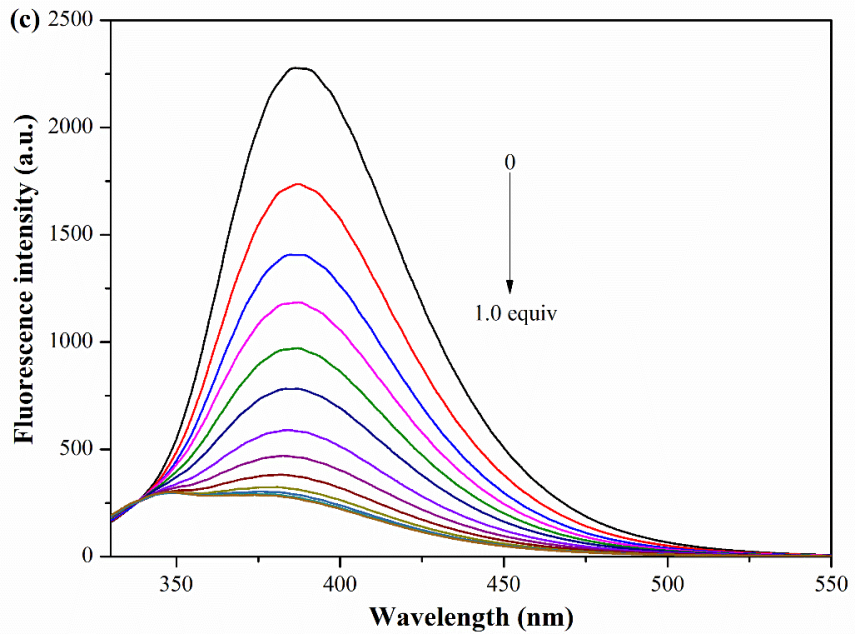

F I G U R E 4 (a) Fluorescence spectra of **H_2L** solution (DMF: H_2O (9:1, V / V)) in the absence and presence of various metal cations (Li^+, Na^+, K^+, Mg^{2+}, Ca^{2+}, Sr^{2+}, Ba^{2+}, Cr^{3+}, Mn^{2+}, Fe^{3+}, Co^{2+}, Ni^{2+}, Cu^{2+}, Zn^{2+}, Pb^{2+}, Ag^+, Cd^{2+}, Al^{3+} and Hg^{2+}). (b) Fluorescence response of the L-Cu^{2+} solution to various metal ions (value at 387nm). λ_{ex} = 330 nm. (c) Fluorometric titration of Cu^{2+} with the probe **H_2L**.

Accepted Article

This article is protected by copyright. All rights reserved.

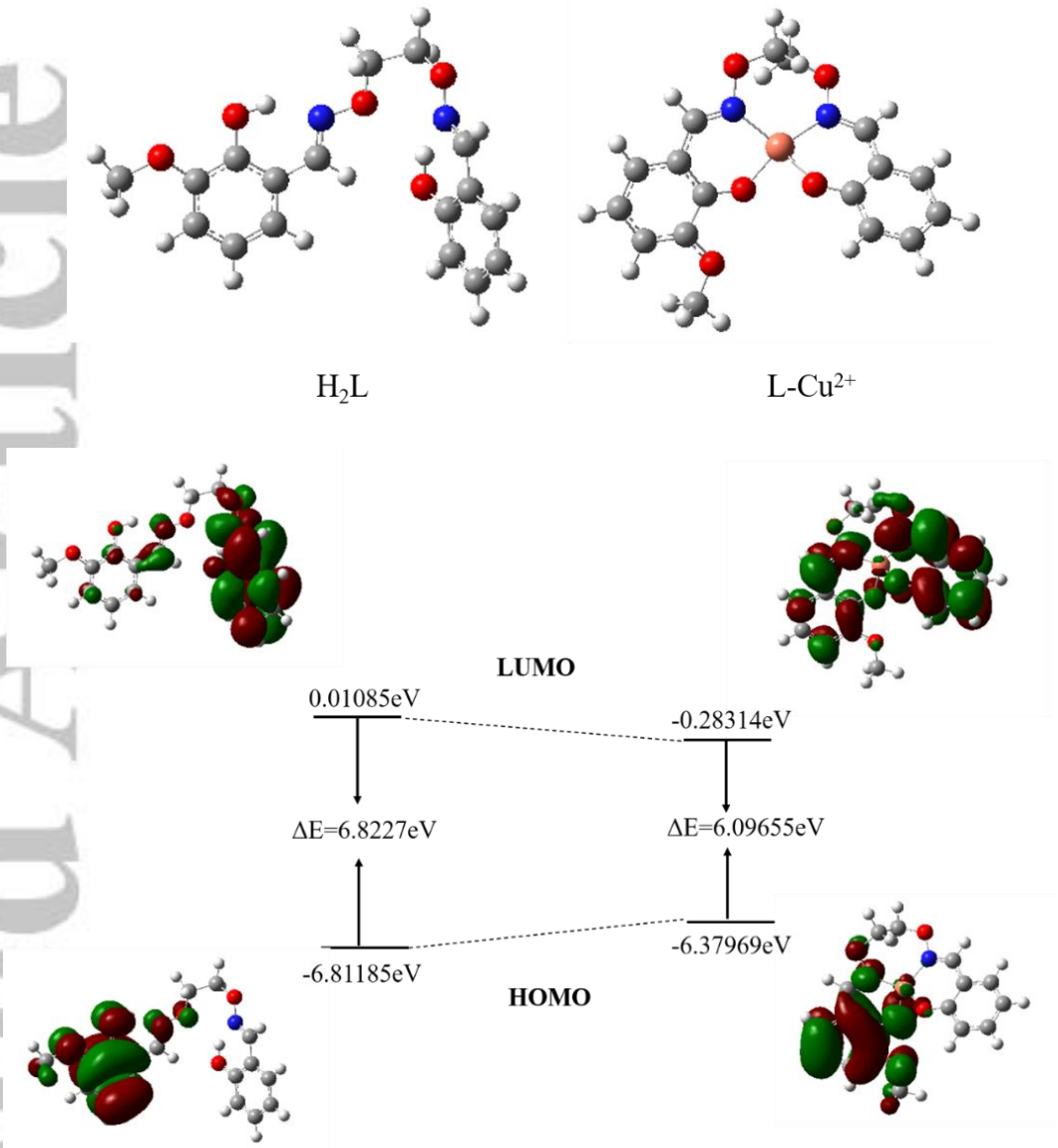

F I G U R E 5 HOMO and LUMO level orbit diagrams of **H_2L** and **L**-Cu^{2+}.

Accepted Article

This article is protected by copyright. All rights reserved.

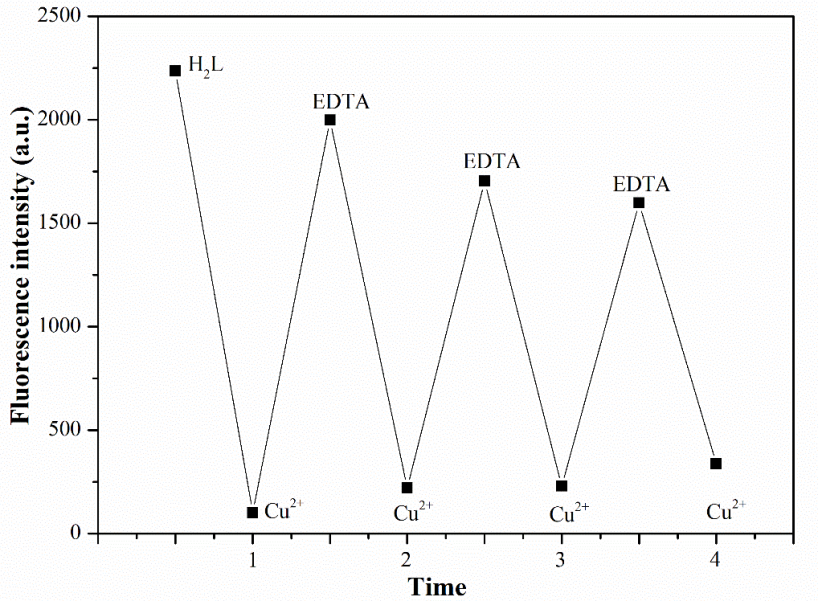

F I G U R E 6 Reversible fluorescence experiment of **H_2L** on Cu^{2+}.

Accepted Article

This article is protected by copyright. All rights reserved.

Accepted Article

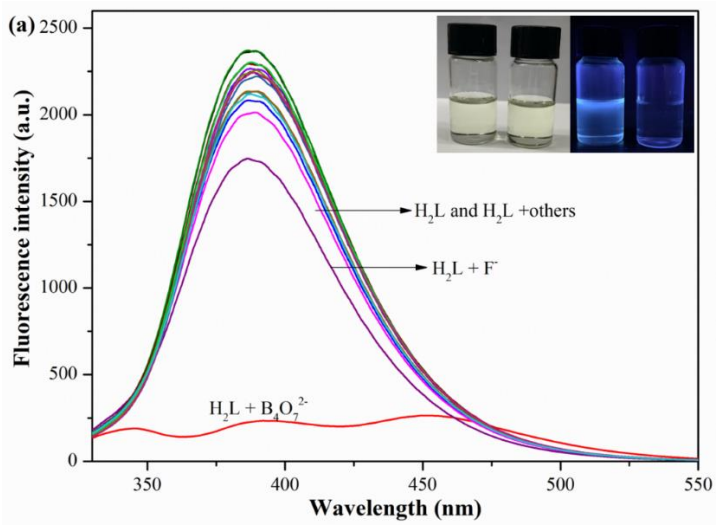

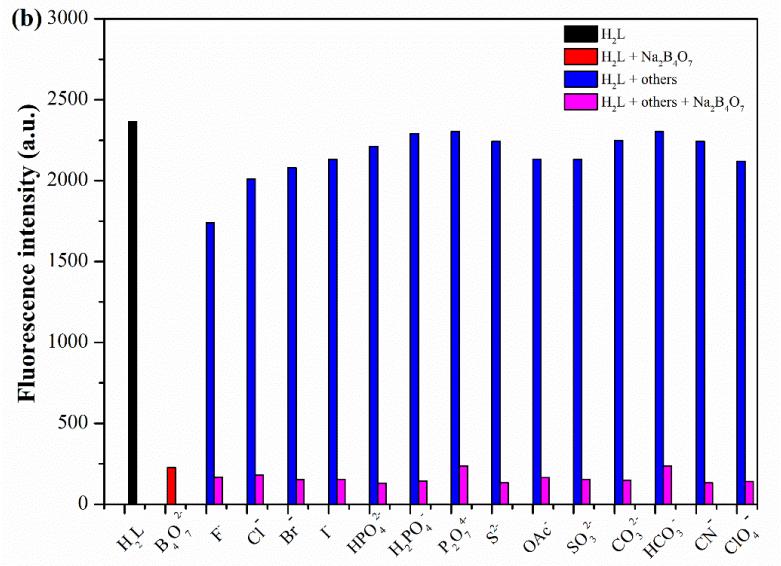

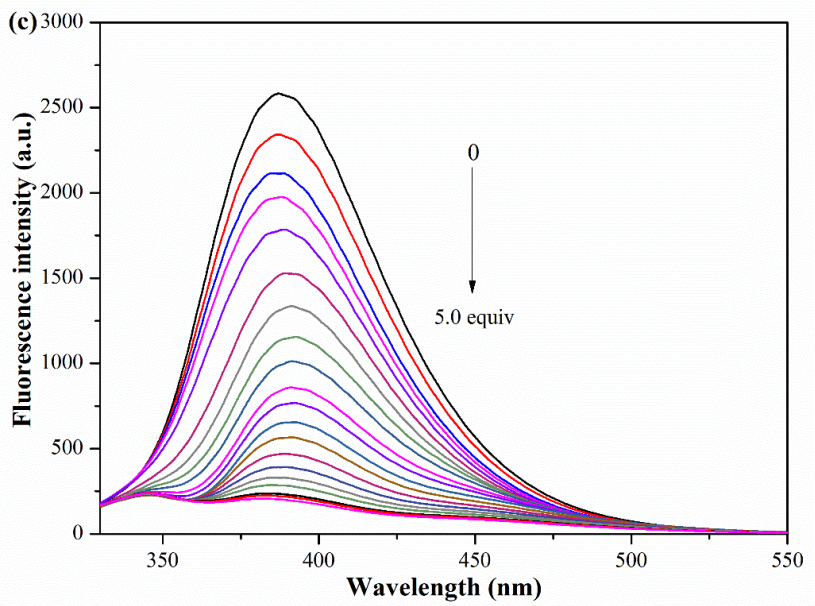

This article is protected by copyright. All rights reserved.

F I G U R E 7 (a) Fluorescence emission spectra of **H_2L** solution in the presence of different anions (F^-, Cl^-, Br^-, I^-, HPO_4^{2-}, $H_2PO_4^-$, $P_2O_7^{4-}$, S^{2-}, OAc^-, SO_4^{2-}, CO_3^{2-}, HCO_3^-, CN^-, ClO_4^- and $B_4O_7^{2-}$). (b) Fluorescence response of L-$B_4O_7^{2-}$ solution to other anions (value at 387nm). λ_{ex} = 330nm. (c) Titration of $B_4O_7^{2-}$ into **H_2L** solution.

Accepted Article

This article is protected by copyright. All rights reserved.

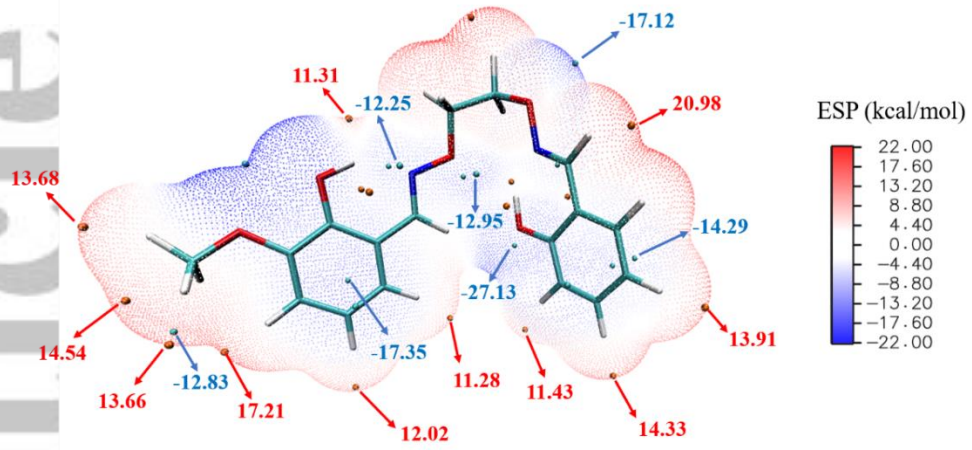

F I G U R E 8 Electrostatic potential (ESP) diagram for **H_2L**.

Accepted Article

This article is protected by copyright. All rights reserved.

Accepted Article

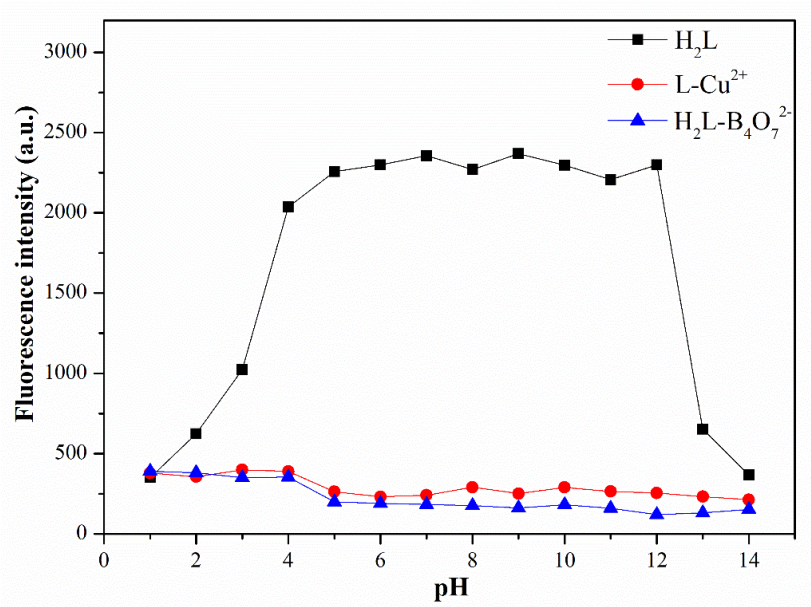

F I G U R E 9 Fluorescence intensity at different pH.

This article is protected by copyright. All rights reserved.

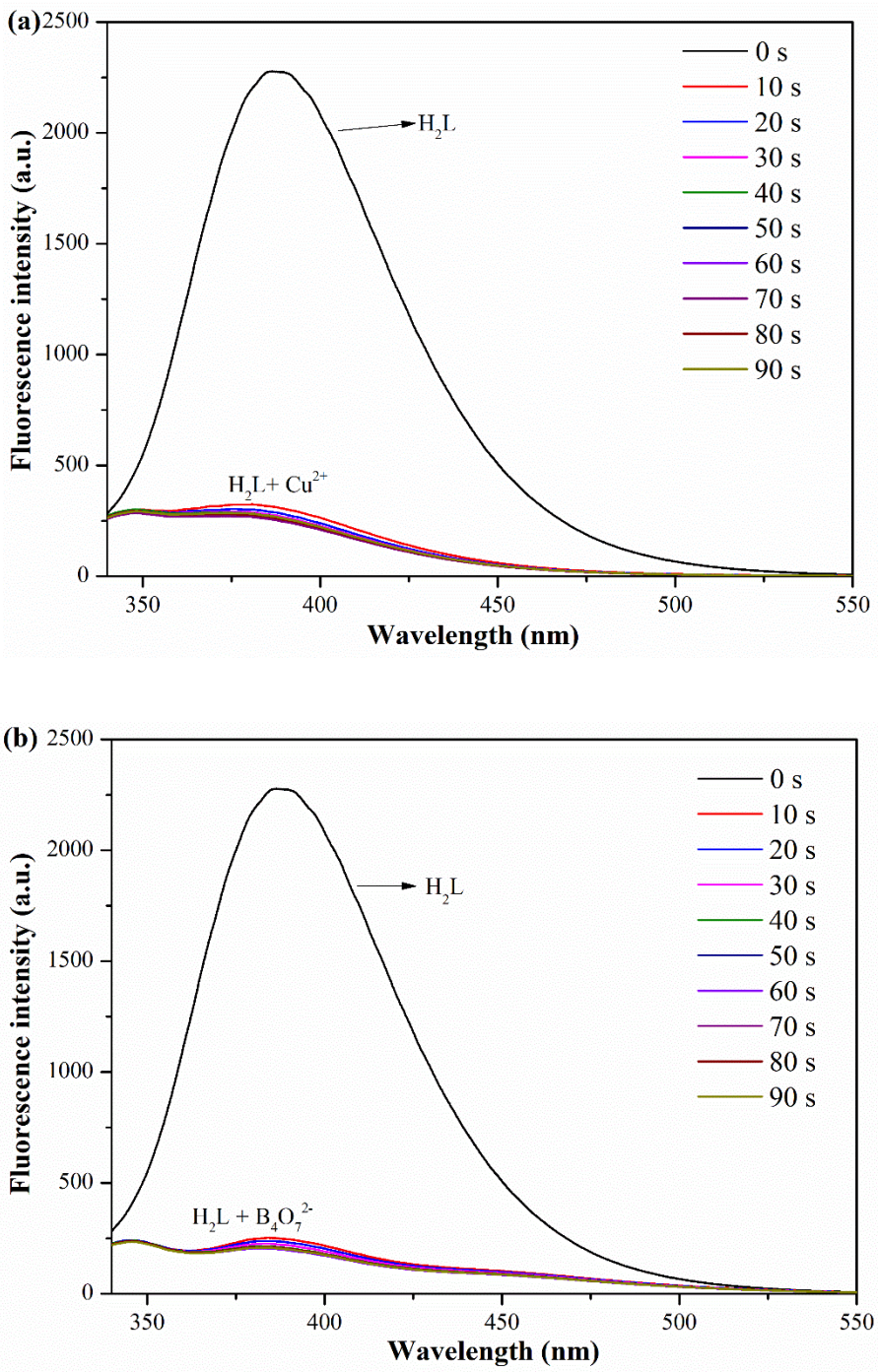

F I G U R E 10 (a) The time response of Cu^{2+} to probe **H_2L**. (b) The time response of $B_4O_7^{2-}$ to probe **H_2L**.

Accepted Article

This article is protected by copyright. All rights reserved.

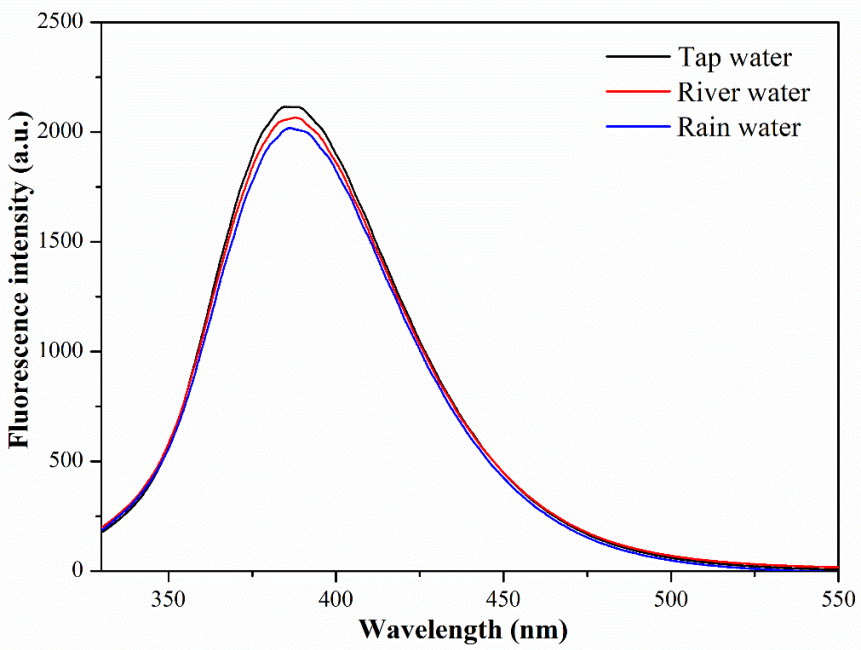

F I G U R E 11 The probe **H_2L** detects the fluorescence intensity of Cu^{2+} in different water samples.

Accepted Article

This article is protected by copyright. All rights reserved.

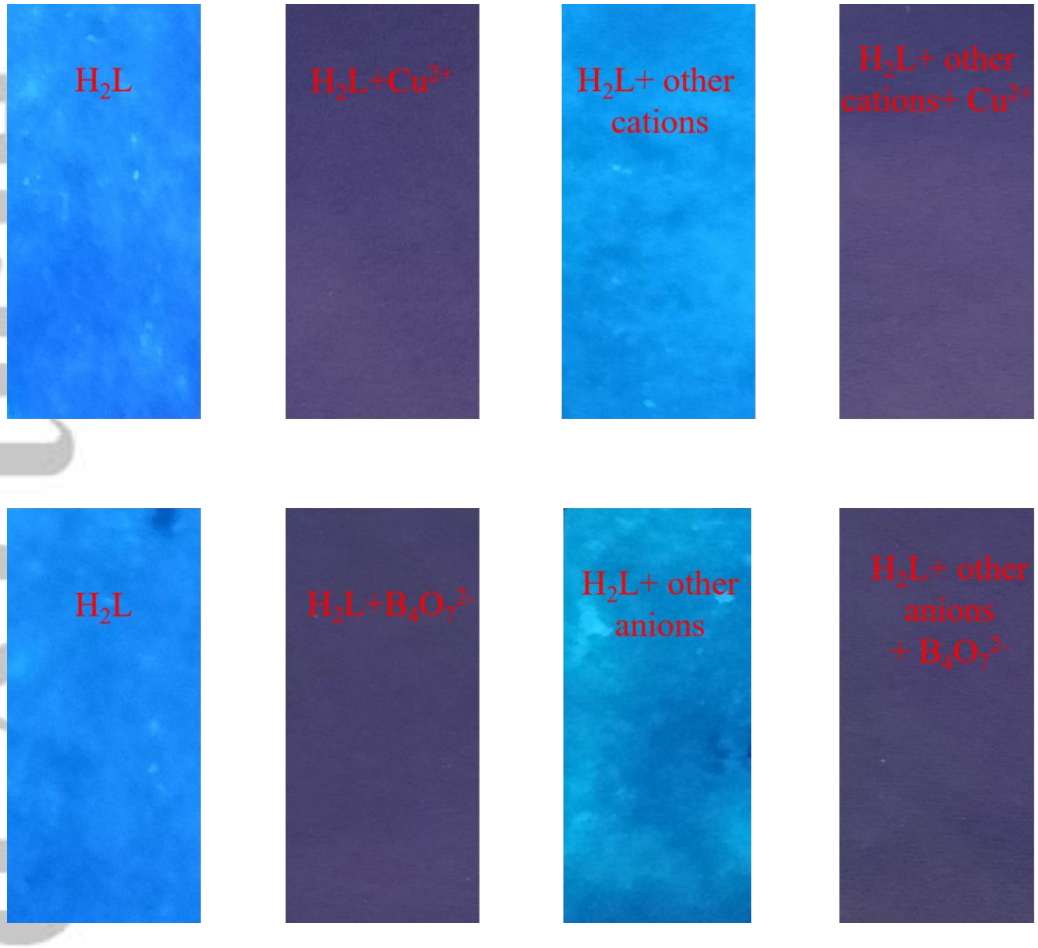

F I G U R E 12 Test paper (Under 365nm UV lamp).

Accepted Article

This article is protected by copyright. All rights reserved.

T A B L E 1 Comparison of binding constants and detection lines between chemosensors.

No.	sensor	Binding constant (M^{-1})	Detection limit (M)	Identification substance	Environmental monitoring	pH range	Reference
1	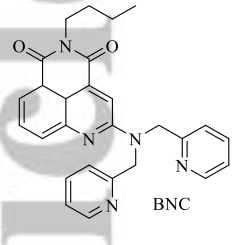 BNC	4.5×10^{3}	4.4×10^{-7}	Cu^{2+}	Lake water	None	[5]
2	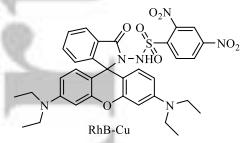 RhB-Cu	6.42×10^{4}	4.7×10^{-6}	Cu^{2+}	Lake water	4~8	[6]
3	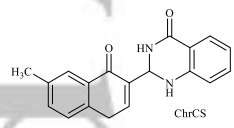 ChrCS	3.27×10^{4}	4.6×10^{-7}	Cu^{2+}	Well water Tab water	1~10	[9]
4	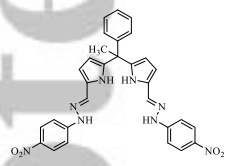	9.82×10^{3}	None	Cu^{2+}	None	None	[10]
5	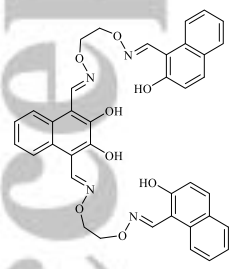	4.72×10^{3}	8.61×10^{-7}	$B_4O_7^{2-}$	None	1~7	[26]
6	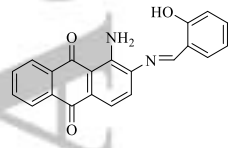	2.51×10^{5}	1.31×10^{-7}	Cu^{2+}	Tap water	7~9	[61]

Accepted Article

This article is protected by copyright. All rights reserved.

7	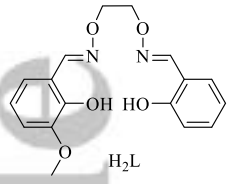	1.36×10^{9}	9.95×10^{-8}	Cu^{2+}	Tap water River water Rain water	4~10	This work
		3.72×10^{8}	4.98×10^{-7}	$B_4O_7^{2-}$	None	4~9	This work

T A B L E 2 Probe **H_2L** to detect different water samples.

Sample	Added Cu^{2+} (μM)	Found (μM)	Recovery (%)	R.S.D. (n = 3) (%)
Tap water	50.0	52.3	104.6	1.3
river water	50.0	55.2	110.4	0.95
rain water	50.0	57.6	115.2	1.1

Accepted Article

This article is protected by copyright. All rights reserved.

Graphical Abstract

The asymmetric salamo-based probe (**H_2L**) was synthesized and structurally characterized. Using high-resolution mass spectrometry and DFT theoretical calculation, it was found that the probe **H_2L** formed a more stable complex (1: 1) with Cu^{2+} to quench its fluorescence, and the probe **H_2L** can also identify $B_4O_7^{2-}$. The probe **H_2L** has the ability to recognize the circulation of Cu^{2+}, and showed a better response in the physiological pH range, and the probe has the characteristics of fast recognition speed and high efficiency. In addition, the probe **H_2L** tested Cu^{2+} and $B_4O_7^{2-}$ test paper, the effect is more obvious. Meanwhile, the probe **H_2L** can be used to quantitatively detect Cu^{2+} in water samples.

Graphical Abstract

Probe for the detection of $Cu^{2+}$and $B_4O_7^{2-}$:

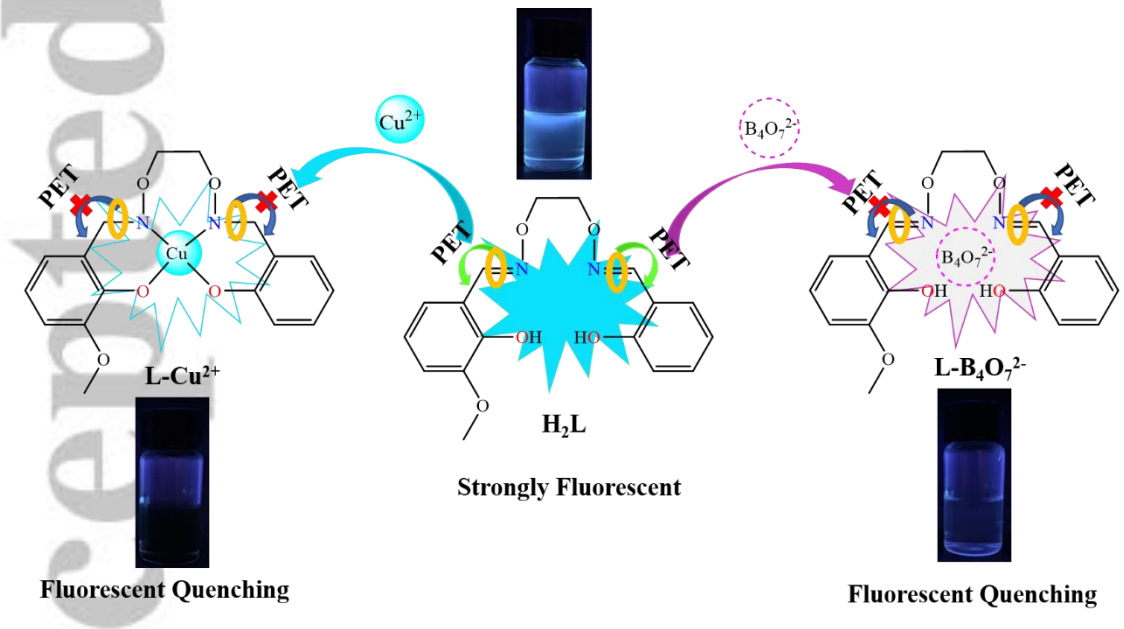

Accepted Article

This article is protected by copyright. All rights reserved.